ORIGINAL ARTICLE

Metal based pharmacologically active agents: Synthesis, structural elucidation, DNA interaction, *in vitro* antimicrobial and *in vitro* cytotoxic screening of copper(II) and zinc(II) complexes derived from amino acid based pyrazolone derivatives

N. Raman [a,*], R. Jeyamurugan [a], S. Sudharsan [a], K. Karuppasamy [a], L. Mitu [b]

[a] *Research Department of Chemistry, VHNSN College, Virudhunagar 626 001, India*
[b] *Department of Chemistry, Faculty of Science, University of Pitesti, Pitesti 110 040, Romania*

Abstract The paper presents the synthesis of complex combinations of Cu(II) and Zn(II) with Schiff base obtained by the condensation reaction of 4-aminoantipyrine with benzaldehyde and 2-amino-3-methyl-butanoicacid. Structural features of synthesized compounds were determined by analytical and spectral techniques. Binding of synthesized complexes with calf thymus DNA (CT DNA) was studied by spectroscopic methods and viscosity measurements. Experimental results indicated the ability of the complexes to form adducts with DNA and to distort the double helix by changing the base stacking. Oxidative DNA cleavage activities of the complexes were studied with supercoiled (SC) pUC19 DNA using gel electrophoresis. The *in vitro* antimicrobial screening effects of the investigated compounds were monitored by the disk diffusion method. The synthesized Schiff base complexes exhibited higher antimicrobial activity than the respective free Schiff base. The *in vitro* cytotoxicity of synthesized complexes against Ehrlich ascites carcinoma (EAC) tumor model

* Corresponding author. Fax: +91 4562 281338.
E-mail address: drn_raman@yahoo.co.in (N. Raman).

was investigated using trypan blue dye exclusion assay. The complexes possessed significant cytotoxic activity.

1. Introduction

Schiff base complexes are considered to be among the most important stereochemical models in main group and transition metal coordination chemistry due to their preparative accessibility and structural variety (Alexander, 1995). Schiff bases are potential anticancer drugs and when administered as their metal complexes, the anticancer activity of these complexes has been enhanced in comparison with the free ligand (Granovskii et al., 1993).

Schiff bases of 4-aminoantipyrine and its complexes present a great variety of biological activity ranging from antitumor, fungicide, bactericide, anti-inflammatory and antiviral activities (Teng et al., 2010; Abdel-Rahman et al., 2010; Santos et al., 2010). Schiff bases of 4-aminoantipyrine has an advantage as it has two potential donor sites and is likely to form three types of compounds with metal ions (Hossain et al., 1996) *viz.* (i) chelates utilizing both donor atoms, (ii) amine salts, using only the amino nitrogen atoms and (iii) two types of complexes, *i.e.*, coordination only from the carbonyl oxygen atom or amino nitrogen atom. Hence, 4-aminoantipyrine is continued to attract considerable attention from theoretical points concerning the mode of binding and their general reactivity as coordinated ligands. Moreover, the number of transition metal complexes with oxygen and nitrogen donor Schiff base derivatives of 4-aminoantipyrine is limited. As of now, only few works describe the synthesis and characterization of these compounds based on aminoantipyrine Schiff bases (Raman et al., 2004, 2007; Selvakumar et al., 2007).

Bearing these facts in mind, we have been tempted to study the synthesis of complex combinations of Cu(II) and Zn(II) with Schiff bases obtained through the condensation of 1-phenyl-2,3-dimethyl-4-aminopyrazol-5-one(4-aminoantipyrine) and 2-amino-3-methyl-butanoicacid. This ligand system has both nitrogen and oxygen donor sites. It is expected that this system coordinates to the metal ion in a tridentate manner through the carboxylate oxygen atom, the nitrogen atom of amino group and the azomethine nitrogen atom of the Schiff base. Carboxylic oxygen atom and amino group are recognized as hard donors which favor the higher oxidation state; the imine function is known to stabilize the lower oxidation state of the metal through π-interaction (Agarwal and Singh, 1986; Radhakrishnan et al., 1984). It is planned to analyze the formation of complexes with Cu(II), and Zn(II) metal ions with various molar ratios. This work also describes the structural features, DNA binding and DNA cleavage studies. Further, this work also deals with the *in vitro* antimicrobial and *in vitro* cytotoxic assays of the synthesized compounds.

2. Experimental

2.1. Materials and reagents

All reagents and chemicals were procured from Merck products. Solvents used for electrochemical and spectroscopic studies were purified by standard procedures (Dickeson and Summers, 1970). DNA was purchased from Bangalore Genei (India). Agarose (molecular biology grade), ethidium bromide (EB) were obtained from Sigma (USA). Tris(hydroxymethyl) aminomethane–HCl (Tris–HCl) buffer solution was prepared using deionized, sonicated triply distilled water. EAC cells were obtained through the courtesy of Amala Cancer Research Centre, Trissur, India. They were maintained by weekly intraperitoneal inoculation of 10^6 cells/mouse (Tweedy, 1964).

2.2. Instruments

Carbon, hydrogen and nitrogen analysis of the complexes were carried out on a CHN analyzer Calrlo Erba 1108, Heraeus. The infrared spectra (KBr disks) of the samples were recorded on a Perkin–Elmer 783 series FTIR spectrophotometer. The electronic absorption spectra in the 200–1100 nm were obtained on a Shimadzu UV-1601 spectrophotometer. ^{1}H and ^{13}C NMR spectra (300 MHz) of the ligand and its zinc complexes were recorded on a Bruker Avance DRX 300 FT-NMR spectrometer using CDCl$_3$ as solvent. Tetramethylsilane was used as internal standard. Fast atomic bombardment mass spectra (FAB-MS) were obtained using a VGZAB-HS spectrometer in a 3-nitrobenzylalcohol matrix. The X-band EPR spectra of the complexes were recorded at RT (300 K) and LNT (77 K) using DPPH as the g-marker. Molar conductance of 10^{-3} M solutions of the complexes in N,N'-dimethylformamide (DMF) were measured at room temperature with an Deepvision Model-601 digital direct reading deluxe conductivity meter. Magnetic susceptibility measurements were carried out by employing the Gouy method at room temperature on powder sample of the complex. CuSO$_4$·5H$_2$O was used as calibrant. Electrochemical measurements were performed on a CHI 620C electrochemical analyzer with three electrode system of a glassy carbon electrode as the working electrode, a platinum wire as auxiliary electrode and Ag/AgCl as the reference electrode. Solutions were deoxygenated by purging with N$_2$ prior to measurements. The metal contents of the complexes were determined according to the literature method (Angellici, 1969). The purity of ligand and its complexes were evaluated by column and thin layer chromatography.

2.3. Synthesis of Schiff base (L)

An ethanolic solution of 4-aminoantipyrine (2.07 g, 10 mM) was added to an ethanolic solution of benzaldehyde (1.06 g, 10 mM). On stirring, the solid product separated was filtered and recrystallized from ethanol.

The hot ethanolic solution (20 mL) of the above solid product (2.8 g, 10 mM) was stirred for *ca.* 4 h with an alkaline ethanolic (0.44 g of NaOH, 11 mM) solution of 2-amino-3-methyl-butanoicacid (1.214 g, 10 mM) and then the mixture was allowed to evaporate at room temperature. The yellow solid crystal formed was recrystallized from ethanol. Yield: 80%. M.P. 204 °C. The outline synthesis of ligand is shown in Scheme 1.

2.4. Synthesis of metal complexes

2.4.1. Synthesis of binuclear copper complex (1)
An ethanolic solution of Schiff base L (0.325 g, 1 mM) was refluxed for *ca.* 4 h with an ethanolic solution of copper sulfate (0.52 g, 2 mM). The solid complex was separated, filtered and washed with ethanol and dried *in vacuo*. Yield: 48%.

2.4.2. Synthesis of copper(II) and zinc(II) complexes with 1:2 metal/ligand ratio
An ethanolic solution of L (0.65 g, 2 mM) was refluxed for *ca.* 4 h with the ethanolic solution of metal salts such as copper(II) chloride (2)/zinc(II) chloride (3) (0.34 g/0.237 g, 1 mM). The solid complexes separated were filtered and washed with ethanol and dried *in vacuo*. Yield: 52% for complex (2) and 58% for complex (3).

2.4.3. Synthesis of copper(II) and zinc(II) complexes with 1:1 metal/ligand ratio
An ethanolic solution of L (0.325 g, 1 mM) was refluxed for *ca.* 4 h with the ethanolic solution of metal salts such as copper(II)

Scheme 1   Outline synthesis of ligand (L).

chloride (4)/zinc(II) chloride (5) (0.34 g/0.237 g, 1 mM). The solid complexes separated were filtered and washed with ethanol and dried *in vacuo*. Yield: 56% for complex (4) and 49% for complex (5).

2.5. DNA binding and cleavage studies

All the DNA binding experiments involving the interaction of the complexes with Calf thymus (CT) DNA were carried out in Tris–HCl buffer (50 mM Tris–HCl, pH 7.2) containing 5% DMF at room temperature. A solution of CT DNA in the buffer gave a ratio of UV absorbance at 260 and 280 nm of about 1.89:1, indicating the CT DNA sufficiently free from protein. The CT DNA concentration per nucleotide was determined by absorption spectroscopy using the molar absorption coefficient of 6600 M^{-1} cm^{-1} at 260 nm (Marmur, 1961).

2.5.1. Absorption spectroscopic studies
Absorption titration experiments were performed by maintaining the metal complex concentration as constant at 50 μM while varying the concentration of the CT DNA within 40–400 μM. While measuring the absorption spectrum, equal quantity of CT DNA was added to both the complex solution and the reference solution to eliminate the absorbance of CT DNA itself. From the absorption data, the intrinsic binding constant K_b was determined from the plot of $[DNA]/(\varepsilon_a - \varepsilon_f)$ versus [DNA] using the following equation:

$$[DNA]/(\varepsilon_a - \varepsilon_f) = [DNA]/(\varepsilon_b - \varepsilon_f) + [K_b(\varepsilon_b - \varepsilon_f)]^{-1}$$
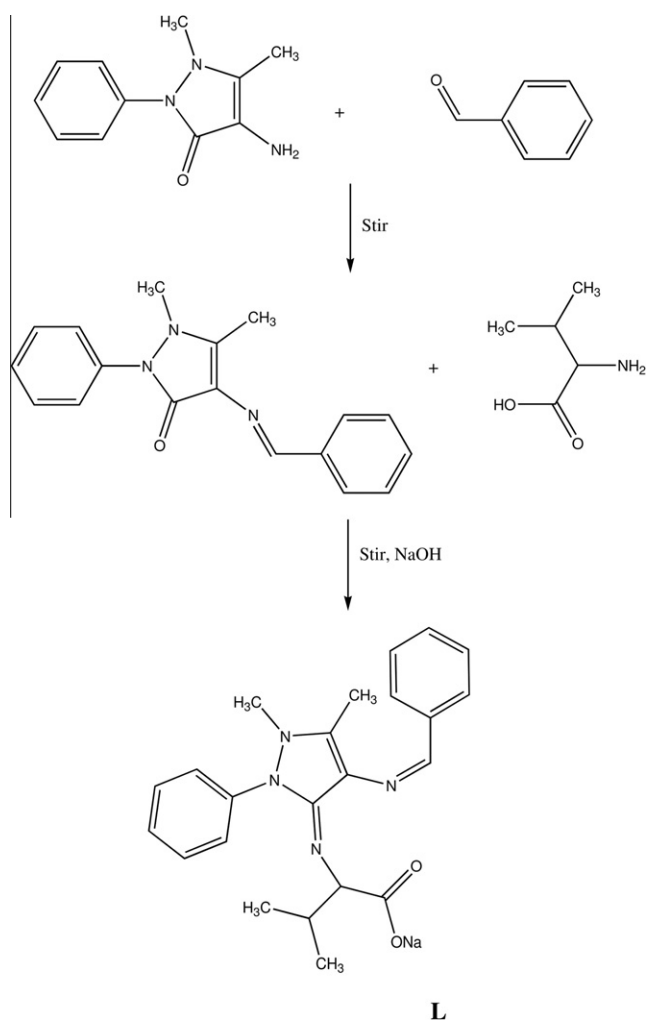
where [DNA] is the concentration of CT DNA in base pairs. The apparent absorption coefficients ε_a, ε_f and ε_b correspond to $A_{obsd}/[M]$, the extinction coefficient for the free metal(II) complex and extinction coefficient for the metal(II) complex in the fully bound form, respectively (Reichmann et al., 1954). K_b is given by the ratio of slope to the intercept.

2.5.2. Electrochemical methods
Cyclic voltammetry and differential pulse voltammogram studies were performed on a CHI 620C electrochemical analyzer with three electrode system of glassy carbon as the working electrode, a platinum wire as auxiliary electrode and Ag/AgCl as the reference electrode. Solutions were deoxygenated by purging with N_2 prior to measurements. The freshly polished glassy electrode was modified by transferring a droplet of 2 μL of 2.5×10^{-3} M of CT DNA solution onto the surface, followed by air drying. Then the electrode was rinsed with distilled water. Thus, a CT DNA-modified glassy carbon electrode was obtained.

2.5.3. Viscosity measurements
Viscosity experiments were carried on an Ostwald viscometer, immersed in a thermostated water-bath maintained at a constant temperature at 30.0 ± 0.1 °C. CT DNA samples of approximately 0.5 mM were prepared by sonication in order to minimize complexities arising from CT DNA flexibility (Charies et al., 1982). Flow time was measured with a digital stopwatch three times for each sample and an average flow time was calculated. Data were presented as $(\eta/\eta^0)^{1/3}$ versus

the concentration of the metal(II) complexes, where η is the viscosity of CT DNA solution in the presence of complex, and η^0 is the viscosity of CT DNA solution in the absence of complex. Viscosity values were calculated after correcting the flow time of buffer alone (t_0), $\eta = (t - t_0)/t_0$ (Satyanarayana et al., 1983).

2.5.4. Gel electrophoresis
DNA cleavage experiment was monitored by agarose gel electrophoresis method. The gel electrophoresis experiment was performed by incubation at 35 °C for 1.5 h as follows: The samples containing SC pUC19 DNA 30 μM, 50 μM copper complex and 500 μM MPA in 50 mM Tris–HCl buffer (pH = 7.2) were electrophoresed for 2 h at 50 V on 1% agarose gel using Tris-boric acid-EDTA buffer (pH = 8.3). After electrophoresis, the gel was stained using 1 μg/cm^3 ethidium bromide (EB) and snapped under UV light.

2.6. Pharmacological studies

2.6.1. In vitro antimicrobial assay
The synthesized ligand and its complexes were tested for their *in vitro* antimicrobial activity against the Gram-positive bacteria *Staphylococcus aureus, Bacillus subtilis*, the Gram-negative bacteria *Escherichia coli, Klebsiella pneumoniae* by the disk diffusion method, using agar nutrient as the medium and against the fungi *Aspergillus niger, Fusarium solani, Curvularia lunata* and *Rhizoctonia bataicola* by disk diffusion method using potato dextrose agar as medium. The stock solution (10^{-2} M) was prepared by dissolving the compounds in DMSO, the solutions were then serially diluted in order to find out the minimum inhibitory concentration (MIC) values. Streptomysin and nystatin were used as control drugs.

2.6.2. Effect of Cu(II) and Zn(II) complexes on in vitro cytotoxicity
Short-term cytotoxicity was assessed by incubating 1×10^6 EAC cells in 1 mL phosphate buffer saline with varying concentrations of the complexes at 37 °C for 3 h in CO$_2$ atmosphere ensured using a McIntosh field jar. The viability of the cells was determined by the trypan blue exclusion method (Sheeja et al., 1997).

2.6.3. Statistical analysis
All values were expressed as mean + SEM. The data were statistically analyzed by one-way ANOVA followed by Dunnett's test, the data of hematological parameters were analyzed using ANOVA followed by Tukey multiple comparison test and data of solid tumor were analyzed using Student's 't' test. P values < 0.05 were considered significant.

3. Results and discussion

The synthesized ligand and its Cu(II) and Zn(II) complexes were found to be air–stable. The ligand was soluble only in common organic solvents. The synthesized complexes were soluble in water, DMF and DMSO. The ligand and its complexes were characterized by the analytical and spectral techniques. Physical characterization, microanalytical, molar conductance and magnetic susceptibility data of the compounds are given in Table. 1.

3.1. Elemental analysis and molar conductance

The analytical data of the complexes (**1**), (**2** and **3**) **and** (**4** and **5**) correspond well with the general formulae of [Cu$_2$L$_2$]SO$_4$, [ML$_2$] and [MLCl] type respectively, where M = Cu(II) and Zn(II); L = Schiff base. The higher molar conductivity of the ligand in water showed the 1:1 electrolytic nature of the ligand, confirming the presence of the ligand in the form of its sodium salt. The observed high molar conductivity of the complex (**1**) in water at room temperature was consistent with the electrolytic nature of the complex while the complexes (**2**), (**3**), (**4**) and (**5**) in water showed low molar conductivity which was consistent with the non-electrolytic nature of the complexes. Elemental analysis results for the metal complexes were in good agreement with calculated values showing that the complexes (**1**), (**2** and **3**) **and** (**4** and **5**) had the metal/ligand ratio of 2:2, 1:2 and 1:1 respectively. Presence of the sulfate ion in the complex (**1**) was evident from the BaCl$_2$ test. Absence of the counter ion (chloride) in the complexes (**2**), (**3**), (**4**) and (**5**) was evident from Volhard's test.

3.2. Mass spectra

The FAB-mass spectra of synthesized ligand and its complexes (**1**) and (**2**) were recorded and the obtained molecular ion peaks confirm the proposed formulae. Mass spectrum of the ligand showed a molecular ion peak (M + 1) at m/z 415 corresponding to $[C_{23}H_{27}N_4O_2Na]^+$ ion. Its complexes (**1**) and (**2**) showed the molecular ion (M + 1) peaks at m/z 1007 and 847 (Fig. 1) respectively which confirmed the stoichiometry as being of [Cu$_2$L$_2$]SO$_4$ and [ML$_2$] type respectively. The observed peaks were in good agreement with their proposed formulae as indicated by the microanalytical data. Thus, the mass spectral data support the conclusions drawn from the analytical and low molar conductivity values.

3.3. IR spectra

The IR spectra provide valuable information regarding the coordinating sites of ligand. The IR spectra of the complexes were compared with that of the free ligand to determine the changes that might have taken place during the complexation. A comparative study of the IR spectra of ligand and its metal complexes reveals that certain peaks are common and therefore, only important peaks, which have been either shifted or newly appeared, are discussed. Spectrum of free Schiff base ligand showed a band of the —C═N— group in the region of 1635 cm^{-1} which was shifted to lower frequencies in the spectra of all the complexes (1615–1605 cm^{-1}) indicating the involvement of —C═N— nitrogen in coordination to the metal ion (Raman et al., 2010). Coordination of the Schiff base to the metal through the nitrogen atom was expected to reduce the electron density in the azomethine link and to lower the v(C═N) vibration. All complexes showed bands in the 1090–1100 cm^{-1} and 700–750 cm^{-1} regions which could be assigned to phenyl ring vibrations. The v_{assym} (COO$^-$) band of free ligand observed at 1610–1590 cm^{-1} was shifted to lower wave number in the spectra of metal complexes *i.e.* 1584–1574 cm^{-1}. The v_{sym} (COO$^-$) band of free ligand observed at 1400 cm^{-1} was shifted to lower wave number in the spectra of metal complexes *i.e.* 1384–1378 cm^{-1}, representing coordination of carboxylic acid group with metal ion through the oxygen atom

Table 1 Physical characterization, analytical, molar conductance, and magnetic susceptibility data of the ligand and its complexes.

Compound	Color	Found (calc) (%)					Λ_m (Ω^{-1} cm^2 mol^{-1})	μ_{eff} (BM)
		M	C	H	N	S		
Ligand	Yellow	5.2 (5.6)	66.3 (66.7)	6.5 (6.6)	13.3 (13.5)	–	43.2	–
(1)	Green	12.1 (12.6)	54.4 (54.9)	5.4 (5.4)	10.8 (11.1)	3.0 (3.2)	47.6	0.68
(2)	Green	7.2 (7.5)	65.0 (65.3)	6.3 (6.4)	12.8 (13.2)	–	5.4	1.94
(3)	Dirty white	7.5 (7.7)	64.8 (65.1)	6.2 (6.4)	12.9 (13.2)	–	6.2	–
(4)	Light green	12.7 (13.0)	56.0 (56.3)	5.5 (5.6)	11.0 (11.4)	–	8.4	2.03
(5)	Dirty White	13.0 (13.3)	55.7 (56.1)	5.3 (5.5)	11.1 (11.4)	–	7.5	–

(Nakamoto, 1986). Assignment of the proposed coordination sites was further supported by the appearance of medium bands at 450–480 cm^{-1} and 420–440 cm^{-1} which could be attributed to the v(M—O) and v(M—N) vibrations respectively.

3.4. Electronic absorption spectra

The electronic absorption spectra are often very helpful in the evaluation of results furnished by other methods of structural investigation. The electronic spectral measurements are used for assigning the stereo chemistries of metal ions in the complexes based on the positions and number of d–d transition peaks.

The electronic absorption spectra of the ligand and its Cu(II) complexes were recorded at room temperature using water as the solvent. The absorptions shown by the ligand at 47,169 cm^{-1}, 36,101 cm^{-1} and 29,498 cm^{-1} are intra-ligand charge transfer transitions, assigned to n-π^* (47,169 cm^{-1}) transition of the carbonyl groups and π–π^* transitions (36,101 cm^{-1} and 29,498 cm^{-1}).

The geometry of the metal complexes had been deduced from its electronic spectra and magnetic moment data of the complexes (Table 2). The complex (1) showed a very low magnetic moment measured at room temperature, 0.68 BM per copper center. The subnormal magnetic moment indicates that the copper centers are strongly coupled by anti-ferromagnetic spin–spin interaction through molecular association of square-planar geometry (Carlin, 1965; Zanello et al., 1987), or indicates the fact that a super exchange inter-action is probably occurs (Lam et al., 1994). The absorption spectra exhibited broad absorption band at 16,286 cm^{-1} specific for most of the complexes of Cu(II) (Lam et al., 1994) and a weak band at 20,408 cm^{-1}. The value of the magnetic moment 1.94 BM of the solid complex (2) indicates the presence of an unpaired electron on Cu(II) ion. The electronic absorption spectrum exhibited an absorption band of medium intensity for the complex (2) at 12,531 cm^{-1} which is attributed to the transition of $^2E_g \rightarrow {}^2T_{2g}$ characteristic to a distorted octahedral geometry.

Also, at room temperature the magnetic moment value (2.03 BM) of the solid complex (4) indicates the presence of an unpaired electron on Cu(II) ion in an ideal square-planar environment (Benzekri et al., 1991). The electronic spectrum of complex (4) showed two weak, low-energy bands at 16,447 and 20,120 cm^{-1} which may be assigned to $^2B_{1g} \rightarrow {}^2A_{1g}$ and $^2B_{1g} \rightarrow {}^2E_g$ transitions, characteristic to a square-planar geometry (Crawford and Hatfield, 1977).

3.5. ^1H NMR spectra

The ^{1}H NMR spectra of the Schiff base and its zinc complexes were recorded in CDCl$_3$ at room temperature. The ^{1}H NMR spectra of the Schiff base and its zinc complexes showed a group of multiple signals corresponding to the aromatic protons at 7.1–7.5 δ and isopropyl protons at 3.5–3.8 δ. The three signals of the Schiff base and its zinc complexes around 2.8–3.1, 3.2–3.5 and 1.7–2.1 δ are assigned to —N—CH—, —CH$_3$ and —N—CH$_3$— protons respectively. The spectrum of the Schiff base exhibited signal at 8.0 δ which is attributed to azomethine proton. The absence of —COOH peak in the ligand confirms that the ligand is in the form of its sodium salt. The azomethine proton peak of the zinc complexes was shifted to downfield region at 8.1 δ compared to the free ligand, suggesting the azomethine nitrogen atom is taking part in complexation with metal ion. Thus, ^{1}H NMR study reinforces the conclusions drawn from the IR spectra.

3.6. EPR spectrum of copper complex

EPR spectroscopy is ideally suited to the study of copper in complexes. The copper-29 nucleus has a nuclear moment and a nuclear spin of 3/2. This gives rise to an easily resolvable characteristic four line spectrum. EPR spectra of complexes (1), (2) and (4) were recorded in DMSO solution at room temperature and at liquid nitrogen temperature. The spectra of the complexes at 300 K showed one intense absorption band at high field, which is due to tumbling motion of the molecules. However, these complexes in the frozen state (77 K) showed four well resolved peaks with low intensities in the low field region and one intense peak in the high field region.

The values of g factors were assessed by the method described by Searl et al., 1961. The g tensor values of Cu(II) complex can be used to derive the ground state. In tetragonal and square-planar complexes the unpaired electron lies in the dx^2–y^2 orbital giving $^2B_{1g}$ as the ground state with the $g_{||} > g_\perp > 2.003$ (Hathaway and Billing, 1970; Drago et al., 1983; Ray and Kauffman, 1990; Djebbar-Sid et al., 1997; Anthonisamy and Murugesan, 1998; Mandal and Mukherjee, 1999). From the observed values for complexes (1), (2) and (4), it is clear that $g_{||} > g_\perp$. These data are in agreement with those obtained from the electronic spectra and confirm the square-planar geometry for complexes (1) and (4), and the tetragonal geometry for complex (2). From the values of the g factors it may be determined the geometric parameter G, representing a measure of the exchange interaction between the Cu(II) centers in the complexes, estimated from the following formula:
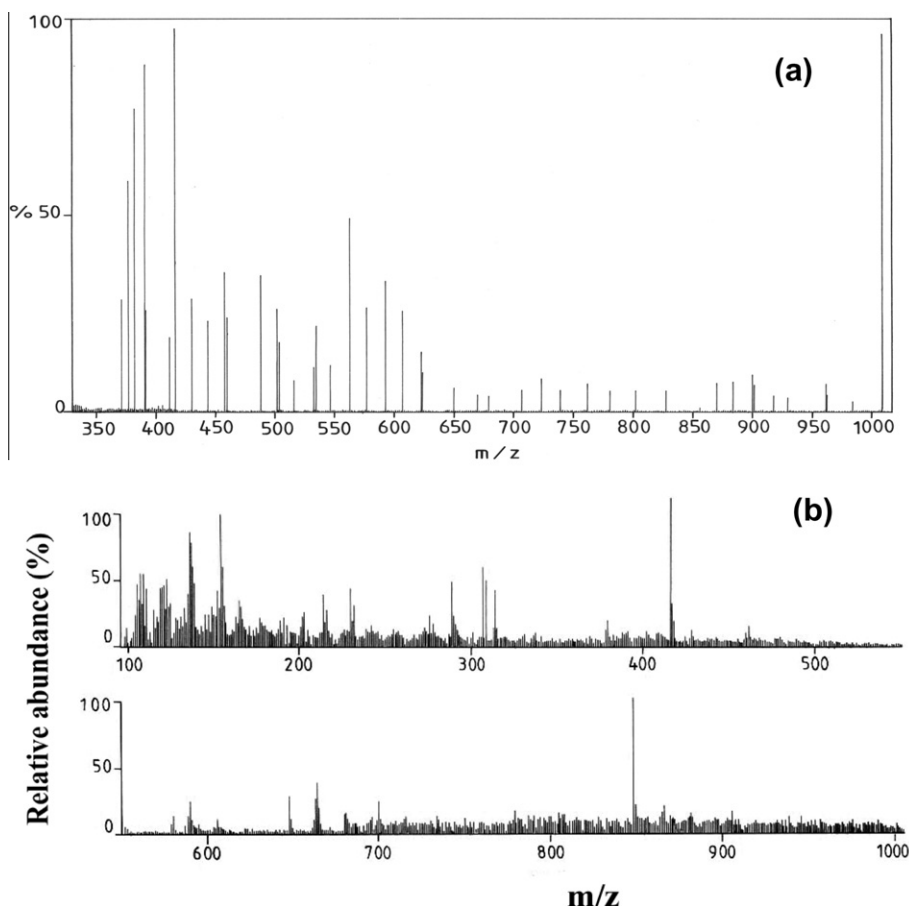
Figure 1 FAB-mass spectra of complexes 1 (a) and 2 (b).

$$G = (g_{\parallel}\text{-}2\text{-}0023)/(g_{\perp} - 2.0023)$$

If $G < 4$, it is considered the existence of some exchange interactions between the Cu(II) centers and if $G > 4$, the exchange interactions are neglected. Thus, in case of complex (**1**), the geometric parameter $G = 2.89$ confirmed the existence of some exchange interactions between the Cu(II) centers. The observed value for the exchange interaction parameter for the complexes (**2**) and (**4**) was greater than 4.0 ($G = 5.4$ for complex (**2**) and 4.3 for complex (**4**)) which confirmed the subsistence of no exchange interactions between the Cu(II) centers. These results were further supported by their magnetic moment values for (**1**), (**2**) and (**4**) as 0.68, 1.94 and 2.03 BM respectively.

Based on the above spectral and analytical data, the proposed structures of the complexes (**1**), (**2** and **3) and (4** and **5**) are given in Figs. 2–4 respectively.

3.7. Electrochemical behavior

The electrochemical properties of the synthesized complexes were studied by cyclic voltammetry in aqueous solution. The cyclic voltammogram of complex (**1**) is shown in Fig. 5. The cyclic voltammogram of the studied complex (**1**) revealed the presence of irreversible cathodic reduction peaks in the -0.312 to -0.518 V range, as it was evident from the fact that the shape and position of a reduction peak changed after the

Table 2 Electronic absorption spectral data of the compounds.

Compound	Absorption (cm^{-1})	Band assignment	Geometry
L	47,169	INCT	
	36,101	INCT	–
	29,498	INCT	
(**1**)	35,224	INCT	
	28,491	INCT	Square-planar
	16,286	$^2B_{1g} \rightarrow {}^2A_{1g}$	
	20,408	$^2B_{1g} \rightarrow {}^2E_g$	
(**2**)	35,425	INCT	Distorted octahedral
	26,846	INCT	
	12,531	$^2E_g \rightarrow {}^2T_{2g}$	
(**3**)	34,659	INCT	–
	28,824	INCT	
(**4**)	34,846	INCT	Square-planar
	29,563	INCT	
	16,447	$^2B_{1g} \rightarrow {}^2A_{1g}$	
	20,120	$^2B_{1g} \rightarrow {}^2E_g$	
(**5**)	35,628	INCT	
	29,003	INCT	–

first cycle. Two observed reduction peaks are assigned to step-wise reduction of the copper(II) ions. The first peak corresponds to the Cu(II)—Cu(II) ↔ Cu(II)—Cu(I), and the second peak to Cu(II)—Cu(I) ↔ Cu(I)—Cu(I) (Mandal et al., 1987). Both reductions are one electron process compared to Cu(II)/Cu(I) process. The difference of the peak positions for the two reductive responses is indicative of the stability of the electro generated Cu(II)—Cu(I) mixed valence state (Fries and Getrost, 1997). A broad anodic oxidation peak was observed for the complex (**1**) in the 0.491 to −0.451 V range. The breadth of the oxidation peak suggests the superposition of two close one-electron processes, which are assigned to the re-oxidation of Cu(II)—Cu(I) and Cu(II)—Cu(II) species, respectively.

The cyclic voltammogram of the complexes (**2**) and (**4**) showed two quasi-redox couples. In the reduction process of complex (**2**), it showed a cathodic peak at 0.384 V for Cu(III)/Cu(II) ($E_{pa} = 0.945$ V, $E_{pc} = 0.384$ V, $\Delta E_p = 0.561$ V, and $E_{1/2} = 0.664$ V). It also showed a cathodic peak at 0.138 V for Cu(II)/Cu(I) ($E_{pa} = 0.791$ V, $E_{pc} = 0.138$ V, $\Delta E_p = 0.653$ V, and $E_{1/2} = 0.464$ V) reduction, consistent with mononuclear complex.

Similarly, in the reduction process of complex (**4**), it showed a cathodic peak at 0.143 V for Cu(III)/Cu(II) ($E_{pa} = 0.492$ mV, $E_{pc} = 0.143$ mV, $\Delta E_p = 0.349$ V, and $E_{1/2} = 0.317$ V). It also showed a cathodic peak at −0.181 V for Cu(II)/Cu(I) ($E_{pa} = -0.742$ V, $E_{pc} = -0.181$ V, $\Delta E_p = -0.561$ V, and $E_{1/2} = -0.461$ V) reduction, consistent with mononuclear complex.

3.8. DNA binding experiments

3.8.1. Electronic absorption titration
Absorption spectrum of the copper complex (**1**) in the absence and in the presence of CT DNA is shown in Fig. 6. With increasing CT DNA concentration, for copper complex, the hypochromism in the band at 368.4 nm reaches 27% with a blue shift of 8.2 nm. These spectral characteristics obviously suggest that the copper complex interacts with DNA most likely through a mode that involves a stacking interaction between the aromatic chromophore and the base pairs of DNA. After intercalating the base pairs of DNA, the π^* orbital of the intercalated ligand can couple with the π orbital of the base pairs thus decreasing the π–π^* transition energy and resulting in bathochromism. On the other hand, the coupling π orbital is partially filled by electrons thus decreasing the transition probabilities and concomitantly resulting in hypochromism. The intrinsic binding constant K_b can be obtained from the ratio of the slope to the intercept of the plots of [DNA]/($\varepsilon_a - \varepsilon_f$) versus [DNA]. To compare quantitatively the affinity of the synthesized complexes towards DNA, the intrinsic binding constants K_b of the synthesized complexes to CT DNA are shown in Table 3. From this table, it is clear that complex (**1**) has higher binding efficacy than other complexes.

3.8.2. Redox behavior
Cyclic and differential pulse voltammetric techniques are extremely useful in probing the nature and mode of DNA binding of metal complexes. Typical cyclic voltammogram of copper complex (**2**) in the absence and in the presence of varying amount of [DNA] is shown in Fig. 7. In the absence of CT DNA, the first redox couple cathodic peak appeared at 0.384 V for Cu(III)/Cu(II) ($E_{pa} = 0.945$ V, $E_{pc} = 0.384$ V, $\Delta E_p = 0.561$ V, and

$E_{1/2} = 0.664$ V) and the second redox couple cathodic peak at 0.138 V for Cu(II)/Cu(I) ($E_{pa} = 0.794$ V, $E_{pc} = 0.138$ V, $\Delta E_p = 0.653$ V, and $E_{1/2} = 0.464$ V). Incremental addition of CT DNA to the complex caused a negative shift in $E_{1/2}$ and an increase in ΔE_p. The i_{pc}/i_{pa} values also decreased in the presence of DNA. The decrease of the anodic and cathodic peak currents of the complex in the presence of DNA is due to the decrease in the apparent diffusion coefficient of the Cu(II) complex upon its complexation with the DNA macromolecule. These results show that the Cu(II) complex stabilizes the duplex (GC pairs) by intercalation. Electrochemical parameters of the synthesized copper complexes are shown in Table 4. These results indicate that the synthesized complexes may stabilize the duplex DNA.

In the absence of CT DNA, the redox couple anodic peak appeared at −0.294 to −0.342 V. Incremental addition of DNA to the Zn(II) complexes showed a decrease in the current intensity and a negative shift of the oxidation peak potential. The resulting changes in the current and potential demonstrate that there is an interaction between Zn(II) and DNA.

Differential pulse voltammogram of the complex (**4**) in the absence and in the presence of varying amount of [DNA] is shown in Fig. 8. An increase in the concentration of DNA caused a negative potential shift along with a significant decrease of the current intensity. The shift in the potential is related to the ratio of the binding constants

$$E_b^{\circ\prime} - E_f^{\circ\prime} = 0.059 \log(K_+/K_{2+})$$

where $E_f^{\circ\prime}$ and $E_b^{\circ\prime}$ are the formal potentials of the, Cu(II)/Cu(I) couple in the free and bound forms, respectively. The ratio of the binding constants (K_{2+}/K_+) for DNA binding of the synthesized complexes were calculated and found to be less than one. The above electrochemical experimental results indicated the preferential stabilization of Cu(II) forms on binding to DNA over other forms.

Differential pulse voltammogram of the presented Zn(II) complex showed a negative potential shift along with a significant decrease of current intensity during the addition of increasing amounts of DNA. This indicates that the zinc ion stabilizes the duplex (GC pairs) by intercalation. Hence, for the complex of the electroactive species (Zn(II)) with DNA, the electrochemical reduction reaction can be divided into two steps.

$$Zn^{2+} - DNA \rightleftharpoons Zn^{2+} + DNA$$

$$Zn^{2+} + 2e^- \rightleftharpoons Zn^0$$
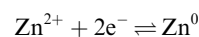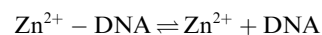
The dissociation constant (K_d) of the Zn(II)-DNA complex was obtained using the following equation (Blackburn and Gait, 1996; Hathaway and Billing, 1970):

$$i_p^2 = \frac{K_d}{[DNA]}\left(i_{p^\circ}^2 - i_p^2\right) + i_{p^\circ}^2 - [DNA]$$

where K_d is dissociation constant of the complex Zn(II)-DNA, $i_{p^\circ}^2$ and i_p^2 are reduction current of Zn(II) in the absence and presence of DNA respectively. The low dissociation constant values (10^{-10} order) of Zn(II) ions were indispensable for structural stability of complexes Zn(II)-DNA which participate in the replication, degradation and translation of genetic material of all species.
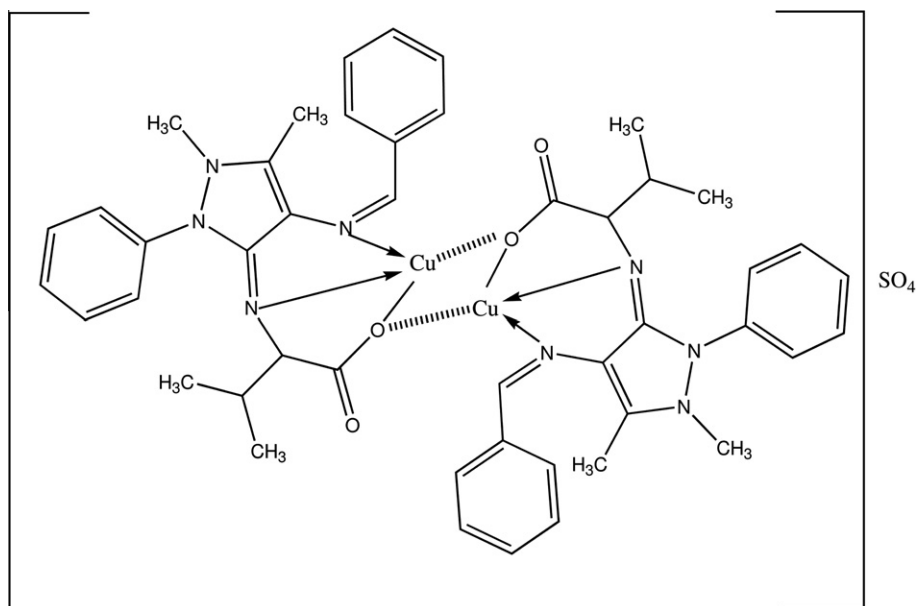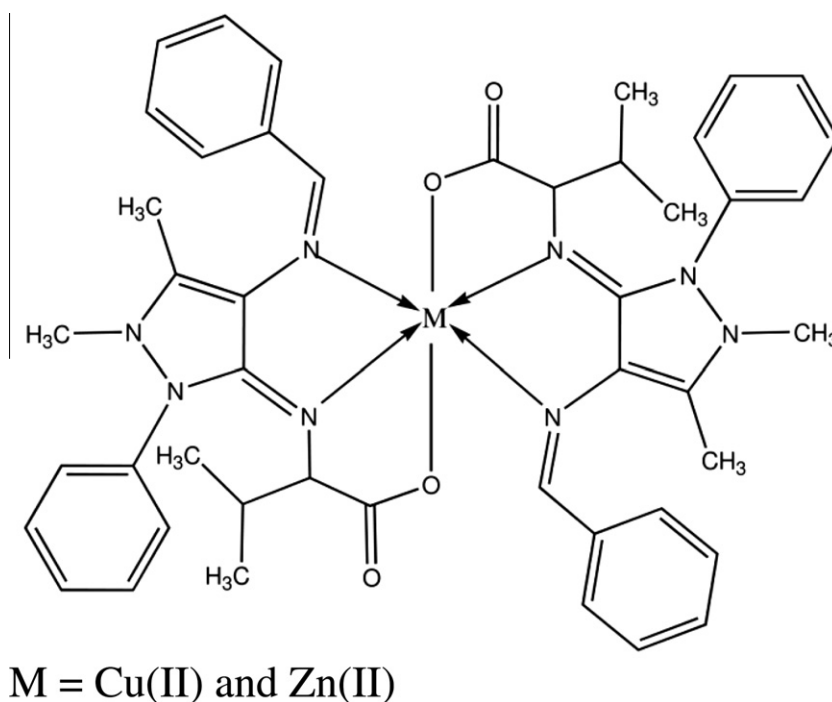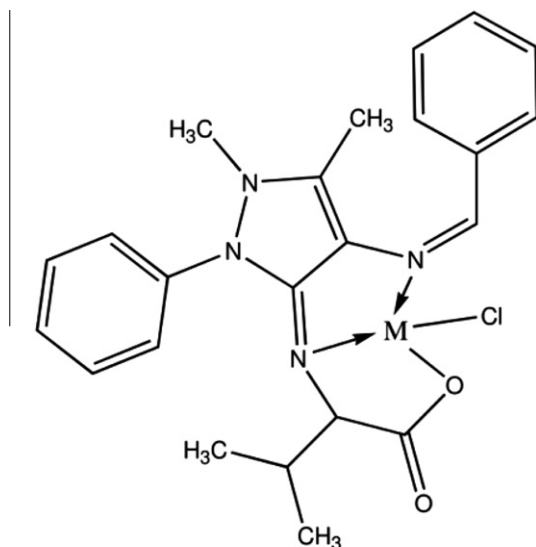
Figure 2 Structure of complex (**1**).

M = Cu(II) and Zn(II)

Figure 3 Structure of complexes (**2** and **3**).

3.8.3. Viscosity measurements

In addition to the peak potential shift in cyclic voltammetry, the spectral shift in UV absorption titration and the dependence of the ionic strength on the binding constant, viscosity measurements were carried out to provide further information on the nature of the interaction between the complex and DNA. A classical intercalation model demands that the DNA helix lengthens as base pairs are separated to accommodate the bound ligand leading to an increase of the DNA viscosity. In contrast, a partial non-classical intercalation of the ligand could bend (or kink) the DNA helix, reduce its effective length and concomitantly also its viscosity in order to further elucidate the binding mode of the present complex. Viscosity measurements were carried out by varying the concentration of the added complex. The effect of the complexes on the viscosity of DNA is shown in Fig. 9. Relative viscosity of DNA increased with the increase in the concentration of the metal complexes, which is similar to that of the classical intercalators (Wang et al., 2007). The viscosity results unambiguously show that complexes bind with DNA in the intercalation mode.

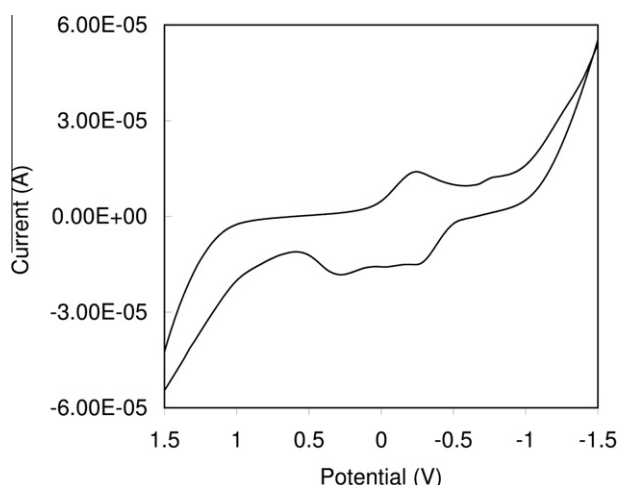M = Cu(II) and Zn(II)

Figure 4 Structure of complexes (**4** and **5**).

Figure 5 Cyclic voltammogram of complex (**1**) in DMF solution; Scan rate 100 mV s^{-1}.

Figure 6 Electronic absorption spectrum of (**1**) in the absence (—) and the presence (—) of increasing amount of CT DNA; R = [NP]/[complex].

3.8.4. Chemical nuclease activity

The DNA cleavage of ligand alone is inactive in the presence and absence of any external agents. The results indicate the importance of the metal in the complex for observing the chemical nuclease activity. Copper complexes can cleave DNA both through hydrolytic and oxidative processes. In the latter instance, these complexes have been shown to react with molecular oxygen or hydrogen peroxide to produce a variety of active oxidative intermediates (reactive oxygen species or ROS), including diffusible hydroxyl radicals and non diffusible copper-oxene species. Normally, a reducing agent like 3-mercaptopropionic acid (MPA) is required to initiate and sustain the radical reaction, but particularly with the employment of DNA derived from biological sources, the presence of an adventitious reducing agent cannot be ruled out. In order to obtain inf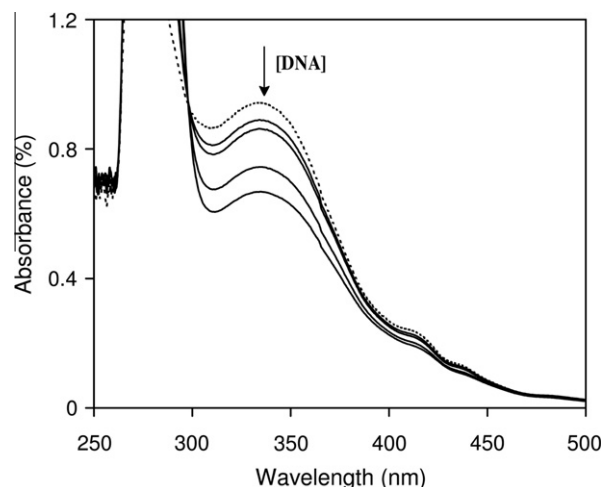ormation about the active chemical species which effect DNA damage, we have looked for the formation of three activated oxygen intermediates: hydroxyl radical, singlet oxygen and superoxide. Figs. 10a and 10b show the influence of the radical scavengers on the DNA cleavage of the copper complexes. From Figs. 10a and 10b, it is evident that the hydroxyl radical scavenger, DMSO, significantly diminished the nuclease activity of copper complexes, which indicates the involvement of the diffusible hydroxyl radical in the cleavage process. Sodium azide, scavenger of singlet oxygen or singlet oxygen-like species, both reduce the DNA damage by introducing the participation of the singlet oxygen or a singlet oxygen-like entity. In fact, the SOD enzyme actually increases the nuclease process, which suggests that in this case the dismutation of the superoxide produced by the enzyme gives rise to ROS which break the DNA strands to a greater extent than the complexes plus reducing agents.

The presence of distamycin, respective binder of the minor groove of DNA, inhibited the breakage of DNA strands, thus implying that complex (**1**) interacts with DNA in the minor groove. But, the complexes (**2**) and (**5**) did not inhibit the cleavage of DNA in the presence of minor groove binder. It indicates that complexes (**2**) and (**5**) interact with DNA in the major groove.

Several possible reaction pathways can account for the cleavage dependent on the presence of hydrogen peroxide. The first step is the interaction of copper(II) complex with DNA through the outer sphere while the second step consists of the reduction of copper(II) complex to copper(I) complex through reaction with the reducing agent. Once copper(I) is formed, a metal-catalyzed Haber–Weis reaction, which makes used of the Fenton chemistry may be considered to be the major mechanism by which the highly reactive hydroxyl radical is generated in biological systems: (Fenton, 1894; Kehrer, 2000)
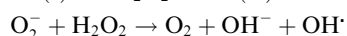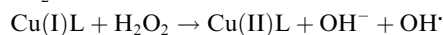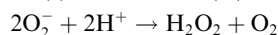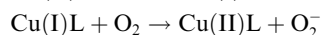
$$Cu(II)L + e^- \rightarrow Cu(I)L$$
$$Cu(I)L + O_2 \rightarrow Cu(II)L + O_2^-$$
$$2O_2^- + 2H^+ \rightarrow H_2O_2 + O_2$$
$$Cu(I)L + H_2O_2 \rightarrow Cu(II)L + OH^- + OH^\cdot$$
$$O_2^- + H_2O_2 \rightarrow O_2 + OH^- + OH^\cdot$$

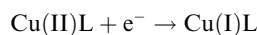**Table 3** Absorption spectral properties of synthesized complexes.

S. no	Complexes	λ_{max} (nm)		$\Delta\lambda$ (nm)	%H	K_b (M^{-1})
		Free	Bound			
1	(1)	368.4	360.2	8.2	27	1.4×10^5
2	(2)	327.0	321.4	5.6	12	1.0×10^4
3	(3)	334.0	332.5	1.5	8	1.2×10^3
4	(4)	346.2	340.1	6.1	5	1.7×10^3
5	(5)	337.0	335.0	2.0	4	0.8×10^3

Figure 8 Redox behavior of complex (4) in the absence (—) and the presence (—) of different concentration of DNA using differential pulse voltammogram; Supporting electrolyte, 50 mM NaCl, 5 mM Tris–HCl, pH = 7.1. Scan rate 100 mV s^{-1}.

Figure 7 Redox behavior of complex (2) in the absence (—) and the presence (—) of different concentration of DNA using cyclic voltammogram; Supporting electrolyte, 50 mM NaCl, 5 mM Tris–HCl, pH = 7.1. Scan rate 100 mV s^{-1}.
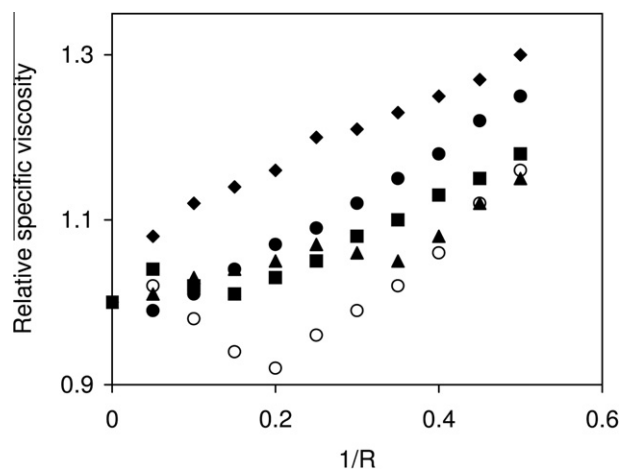
Figure 9 Ratio of the specific viscosity of DNA in the presence of complex to that of free CT DNA versus 1/R (=[Complex]/[NP]) in the presence of complexes (1) (♦), (2) (▲), (3) (○), (4) (●) and (5) (■).

Hydrogen peroxide can also react with another equivalent of Cu(I)L to produce hydroxyl radical-species which could be metal bound. This species, which may be considered analogous to a metal-oxo system, is responsible for initiating DNA strand scission chemistry (Sigman, 1986).

Although the cleavage reaction through zinc complexes does not require additional external agents, we carefully investigated the possibility that diffusible OH radical, singlet oxygen ($^1O_2$) or superoxide anion radical were involved in this reaction. The cleavage efficiency does not change in the presence of DMSO as potential OH radical scavenger, NaN$_3$ as potential $^1O_2$ inhibitor, or SOD as a superoxide anion radical inhibitor (Cheng et al., 1993; Lesko et al., 1980; Khan, 1976). In conclusion, the results presented here rule out the

involvement of any oxidation inhibitors in the strand cleavage, and this reaction most probably occurs through a hydrolytic mechanism. Moreover, experiments support this assumption.

Table 4 Electrochemical parameters of interaction of copper complexes with CT DNA.

| S. no.	Complexes	Redox couple	ΔE_p (V)		$E_{1/2}$ (V)		Decrease of i_{pc} (%)	i_{pa}/i_{pc}		K_+/K_{2+}
			Free	Bound	Free	Bound		Free	Bound	
1	(1)	Cu(II)—Cu(II) ↔ Cu(II)—Cu(I)	0.703	0.681	0.351	0.314	38	0.98	0.93	0.15
		Cu(II)—(Cu(I) ↔ Cu(I)—Cu(I)	−0.067	0.531	−0.484	0.424	31	0.97	0.92	0.17
2	(2)	Cu(III)/Cu(II)	0.561	0.653	0.664	0.464	27	0.94	0.92	1.21
		Cu(II)/Cu(I)	0.432	0.531	0.651	0.546	25	0.93	0.91	0.62
3	(4)	Cu(III)/Cu(II)	0.349	0.356	0.317	0.313	4	0.89	0.88	1.14
		Cu(II)/Cu(I)	0.561	0.597	−0.461	−0.397	28	0.98	0.91	0.58
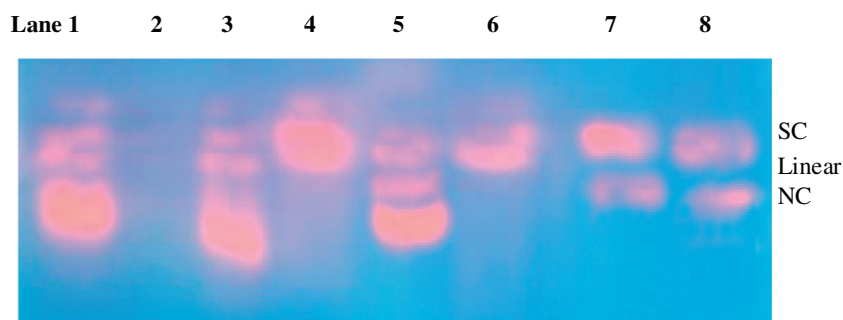
Figure 10a Gel electrophoresis diagram showing the cleavage of SC pUC19 DNA (0.2 µg) by the synthesized complexes (50 µM) in the presence of oxidant (5 mM): lane 1, DNA + (**1**) + H_2O_2; lane 2, DNA + (**1**); lane 3, DNA + (**1**) + distamycin; lane 4, DNA + (**1**) + DMSO (4 µL); lane 5, DNA + (**1**) + MPA + SOD (1 U); lane 6, DNA + (**2**); lane 7, DNA + (**2**) + H_2O_2 + MPA; lane 8, DNA + (**2**) + MPA + distamycin (50 µM).

It is well known that in DNA hydrolytic cleavage 3′-OH and 5′-OPO$_3$ (5′-OH and 3′-OPO$_3$) fragments remain intact and that these fragments can be enzymatically ligated and end-labeled. Fig. 11 shows that the linear DNA fragments cleaved by zinc complexes can be relegated by T4 ligase just like the linear DNA mediated by *Eco*R1. Hence, this result implied that the process of DNA cleavage by the complex occurs *via* a hydrolytic path.

3.9. Pharmacological studies

3.9.1. Antimicrobial assay
The synthesized ligand and their complexes were tested for their *in vitro* antimicrobial activity against the Gram-positive bacteria *S. aureus, B. subtilis*, the Gram-negative bacteria *E. coli, K. pneumoniae* by the disk diffusion method, using agar nutrient as the medium and fungi *A. niger, F. solani, C. lunata* and *R. bataicola* by well diffusion method using potato dextrose agar as medium. Tables 5 and 6 summarize the minimum inhibitory concentration (MIC) values of the investigated compounds. It is clear from the tables that the observed MIC values indicate that most of the complexes have higher antimicrobial activity than the free ligand (L). This is the result of the coordinated metal which plays a significant role for the

antibacterial activity. The chelation theory explains that a decrease in the polarizability of the metal can change the lipophilicity or hydrophobicity of complexes. These properties are now seen as important parameters related to membrane permeation in biological systems. Many of the processes of drug disposition depend on the ability or inability to cross membranes and hence there is a high correlation with measures of lipophilicity. Moreover, many of the proteins involved in drug disposition have hydrophobic binding sites, further adding to the importance of lipophilicity.

By consideration of the structures of compounds that exhibit antimicrobial activity, it can be concluded that the metal moiety may play a role in determining the antibacterial activity. From the results which indicated that the tested compounds were more active against Gram-positive than Gram-negative bacteria, it may be concluded that the inhibitory activity of the studied compounds is related to the cell wall structure of the bacteria. This is possible because the cell wall is essential to the survival of bacteria and some antibiotics are able to kill bacteria by inhibiting a step in the synthesis of peptidoglycan. Gram-positive bacteria possess a thick cell wall containing many layers of peptidoglycan and teichoic acids, but in contrast, Gram-negative bacteria have a relatively thin cell wall consisting of a few layers of peptidoglycan surrounded by a
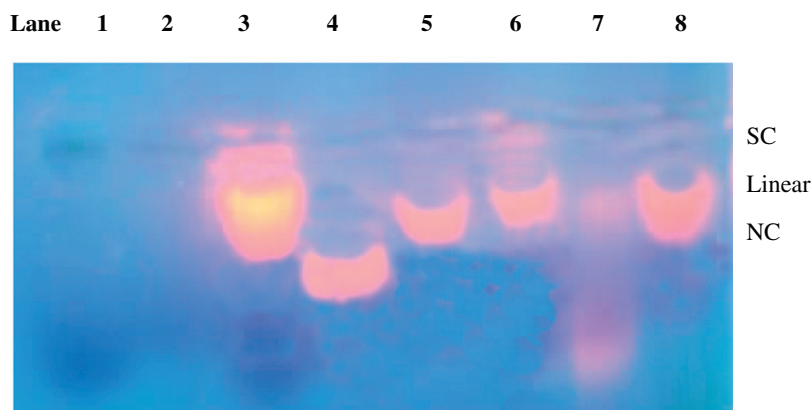

Figure 10b Gel electrophoresis diagram showing the cleavage of SC pUC 19 DNA (0.2 µg) by the synthesized complexes (50 µM) in the presence of MPA (5 mM): lane 1, DNA control; lane 2, DNA + L (50 µM); lane 3, DNA + (**5**) + MPA; lane 4, DNA + (**5**); lane 5, DNA + (**5**) + DMSO (4 µL) + MPA; lane 6, DNA + (**5**) + NaN$_3$ + MPA; lane 7, DNA + (**3**) + distamycin (50 µM) + MPA; lane 8, DNA + (**5**) + MPA + SOD (1 U).
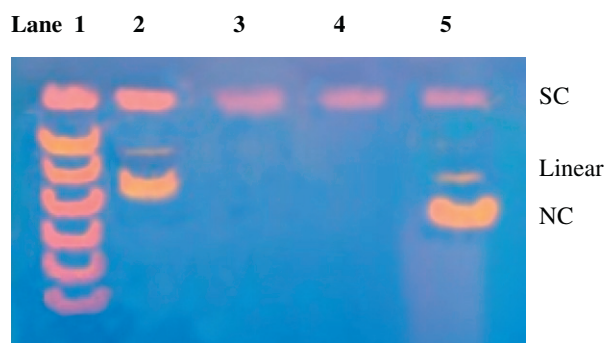
Figure 11 Gel electrophoresis diagram for ligation of SC pUC19 DNA linearized by zinc complex: lane 1, DNA markers; lane 2, DNA + (**3**); lane 3, DNA + (**3**) + T4 DNA ligase; lane 4, DNA + (**3**) + EcoR1; lane 5, DNA + (**3**) + EcoR1 + T4 DNA ligase.

Table 5 Minimum inhibitory concentration of the synthesized compounds against the growth of bacteria.

S. no.	Compound	Minimum inhibitory concentration (MIC) ($\times 10^4$ μM)			
		Staphylococcus aureus	*Bacillus subtilis*	*Escherichia coli*	*Klebsiella pneumoniae*
1	L	18.2	19.5	22.0	25.6
2	(**1**)	1.1	1.3	7.0	7.9
3	(**2**)	1.5	1.9	8.1	7.4
4	(**3**)	1.3	1.8	9.0	8.3
5	(**4**)	1.7	2.0	7.3	7.7
6	(**5**)	1.9	2.3	8.7	7.1
7	Streptomycin	1.7	2.5	1.3	2.0

Table 6 Minimum inhibitory concentration of the synthesized compounds against the growth of fungi.

S. no.	Compound	Minimum inhibitory concentration (MIC) ($\times 10^4$ μM)			
		Aspergillus niger	*Fusarium solani*	*Curvularia lunata*	*Rhizoctonia bataicola*
1	L	26.6	27.5	28.6	29.7
2	(**1**)	1.1	1.4	1.3	1.8
3	(**2**)	1.6	1.7	1.7	1.9
4	(**3**)	1.7	1.9	1.4	1.9
5	(**4**)	1.4	1.6	1.5	1.6
6	(**5**)	1.2	1.8	1.0	1.5
7	Nystatin	1.0	1.7	0.9	1.5

second lipid membrane containing lipopolysaccharides and lipoproteins. These differences in cell wall structure can produce differences in antibacterial susceptibility and some antibiotics can kill only Gram-positive bacteria and is ineffective against Gram-negative pathogens (Shakir et al., 1995).

3.9.2. Effect of Cu(II) and Zn(II) complexes on cytotoxicity in vitro

The short term *in vitro* cytotoxicity study of EAC-bearing mice showed the GI_{50} of complexes to be 100, 200, 300, 400 and 500 μg/mL. The GI_{50} values for all of the complexes are given

Table 7 *In vitro* cytotoxic activity of synthesized complexes in EAC cell line.

Treated compounds	GI_{50} (μg/mL)[a]
(1)	111.31
(2)	125.71
(3)	124.42
(4)	115.27
(5)	114.18
5-FU	110.12

[a] Average of three determinations, three replicates GI_{50}, drug concentration inhibiting 50% cellular growth following 3 h of drug exposure.

in Table 7. All of the complexes tested, (**1**) has lowest GI_{50} value of 111.31 compared to the standard 5-FU (110.12 μg/mL). From this result (**1**) complex has higher cytotoxicity effect on EAC cancer cell line than other complexes. The cytotoxicity order of the complexes is in the following order: (**1**) > (**4**) ≈ (**5**) > (**2**) ≈ (**3**).

4. Conclusions

The Schiff base ligand has been prepared by the condensation of benzaldehyde and 4-aminoantipyrine with 2-amino-3-methyl-butanoicacid. It has been characterized by microanalytical data, IR, UV–Vis., ^{1}H NMR and mass spectra. Its complexes of Cu(II) and Zn(II) have been synthesized and characterized by microanalytical data, IR, UV–Vis. and mass spectra. The data show that they have composition of the type [Cu$_2$L$_2$] SO$_4$, [ML$_2$] and [MLCl] where M = Cu(II) and Zn(II). The UV–Vis., magnetic susceptibility and EPR spectral data of the complexes suggest an distorted octahedral geometry for [ML$_2$] type complexes and square-planar geometry for [Cu$_2$L$_2$]-SO$_4$ and [MLCl] complexes around the central metal ion. The lower electrical conductance values of the complexes reveals that these chelates are non electrolytes. Their magnetic susceptibility values provide evidence for the monomeric nature of [ML$_2$] and [MLCl] type complex and dimeric nature for [Cu$_2$L$_2$]SO$_4$. Electronic absorption, cyclic voltammogram, differential pulse voltammogram and viscosity studies prove that the complexes are interacting with DNA through intercalation. Gel electrophoresis experiments have been carried out on the interaction of the complexes with DNA. The results suggest that all the complexes can cleave DNA. However, zinc complexes cleave DNA by hydrolytic way which is supported by the evidence from free radical quenching and T4 ligase ligation. *In vitro* antimicrobial activities of the compounds have been tested against bacterial and fungal strains using the disk diffusion method. The MIC values against the growth of microorganisms are much larger for metal chelates than the ligand. *In vitro* cytotoxicity of synthesized complexes against Ehrlich ascites carcinoma (EAC) tumor model was investigated using trypan blue dye exclusion assay. The cytotoxicity order of the complexes is in the order of (**1**) > (**4**) ≈ (**5**) > (**2**) ≈ (**3**).

References

Abdel-Rahman, A.A.H., Ahamed, A.H.A., Ramiz, M.M.M., 2010. Chem. Heterocycl. Comp. 46, 72.

Agarwal, R.K., Singh, G., 1986. Synth. React. Inorg. Metal Org. Chem. 16, 1183.

Alexander, V., 1995. Chem. Rev. 95, 273.

Angellici, R.J., 1969. Synthesis and Techniques in Inorganic Chemistry. W.B. Saunders Company.

Anthonisamy, V.S.X., Murugesan, R., 1998. Chem. Phys. Lett. 287, 353.

Benzekri, A., Dubourdeaux, P., Latour, J.M., Rey, P., Laugier, J., 1991. Dalton Trans., 3359.

Blackburn, G.M., Gait, M.J., 1996. Nucleic Acid in Chemistry and Biology, second ed. Oxford University Press, New York.

Carlin, R.L., 1965. Transition Metal Chemistry, second ed. Marcel Decker, New York.

Charies, J.B., Dattagupta, N., Crothers, D.M., 1982. Biochemistry 21, 3933.

Cheng, C.C., Rokita, S.E., Burrows, C.J., 1993. Angew. Chem., Int. Ed. Engl. 32, 277.

Crawford, V.H., Hatfield, W.E., 1977. Inorg. Chem. 16, 1336.

Dickeson, J.E., Summers, L.A., 1970. Aust. J. Chem. 23, 1023.

Djebbar-Sid, S., Benali-Baitich, O., Deloume, J.P., 1997. Polyhedron 16, 2175.

Drago, R.S., Desmond, M.J., Corden, B.B., Miller, K.A., 1983. J. Am. Chem. Soc. 105, 2287.

Fenton, H.J.H.J., 1894. J. Chem. Soc. 65, 899.

Fries, J., Getrost, H., 1997. Organic Reagents for Trace Analysis. E. Merck, Darmstadt, 104.

Granovskii, A.D., Nivorozhkin, A.L., Minkin, V.I., 1993. Coord. Chem. Rev. 126, 1.

Hathaway, B.J., Billing, D.E., 1970. Coord. Chem. Rev. 5, 143.

Hossain, M.E., Alam, M.N., Begum, J., Akbar, A.M., Nazimuddin, M., Smith, F.E., Hynes, R.C., 1996. Inorg. Chim. Acta 249, 207.

Kehrer, J.P., 2000. Toxicology 149, 43.

Khan, A.U., 1976. J. Phys. Chem. 80, 2219.

Lam, F., Wang, R.J., Mak, T.C.W., Chan, K.S., 1994. J. Chem. Soc. Chem. Commun., 2439.

Lesko, S.A., Lorentzen, R.J., Tso, P.O.P., 1980. Biochemistry 19, 3023.

Mandal, S., Mukherjee, R.N., 1999. Dalton Trans., 4025.

Mandal, S.K., Thompson, L.K., Nag, K., Charland, J.P., Gabe, E.J., 1987. Inorg. Chem. 26, 1391.

Marmur, J., 1961. J. Mol. Biol. 3, 208.

Nakamoto, K., 1986. Infrared and Raman Spectra of Inorganic and Coordination Compounds, fourth ed. John Wiley and Sons, New York.

Radhakrishnan, P.K., Indrasenan, P., Nair, C.G.R., 1984. Polyhedron 3, 67.

Raman, N., Kulandaisamy, A., Thangaraja, C., 2004. Trans. Metal Chem. 29, 129.

Raman, N., Dhaveethu Raja, J., Sakthivel, A., 2007. J. Chem. Sci. 119, 303.

Raman, N., Jeyamurugan, R., Rajkapoor, B., Mitu, L., 2010. Spectrochim. Acta, Part A, Mol. Biomol. Spectrosc. 75, 88.

Ray, R.K., Kauffman, G.R., 1990. Inorg. Chem. Acta 173, 207.

Reichmann, M.E., Rice, S.A., Thomas, C.A., Doty, P., 1954. J. Am. Chem. Soc. 76, 3047.

Santos, P.M., Anutunes, A.M., Noronha, J., Fernandes, E., Vieira, A.J., 2010. Eur. J. Med. Chem. 45, 2258.

Satyanarayana, S., Daborusak, J.C., Charies, J.B., 1983. Biochemistry 32, 2573.

Searl, J.W., Smith, R.C., Wyard, S.J., 1961. Proc. Phys. Soc. 78, 1174.

Selvakumar, P.M., Suresh, E., Subramanian, P.S., 2007. Polyhedron 26, 749.

Shakir, M., Varkey, S.P., Nasman, O.S.M., 1995. Polyhedron 14, 1283.

Sheeja, K.R., Kuttan, G., Kuttan, R., 1997. Amala Res. Bull. 17, 73.

Sigman, D.S., 1986. Acc. Chem. Res. 19, 180.

Teng, Y., Liu, R., Yan, S., Pan, X., Zhang, P., Wang, M., 2010. J. Fluores. 20, 381.

Tweedy, B.G., 1964. Phytopathology 55, 910.

Wang, Q.H., Jiao, K., Liu, F.Q., Yuan, X.L., Sun, W., 2007. J. Biochem. Biophys. Methods 70, 427.

Zanello, P., Tamburini, S., Vigato, P.A., Mazzocchin, G.A., 1987. Coord. Chem. Rev. 77, 165.